Journal of Molecular Structure 985 (2011) 120–127

Contents lists available at ScienceDirect

Journal of Molecular Structure

journal homepage: www.elsevier.com/locate/molstruc

Synthesis, spectroscopic and DFT investigation of dimethyl-2-(5-acetyl-2,2-dimethyl-4,6-dioxo-1,3-dioxan-5-yl)-3-(triphenylphosphinylidene)succinate

E. Vessally [a], E. Fereyduni [b,*], Y. Erdogdu [c], A. Habibi [b], K. Eskandari [b], M.T. Gulluoglu [c]

[a] Payame Noor University (PNU), Zanjan, Iran
[b] Faculty of Chemistry, Tarbiat Moallem University, Tehran, Iran
[c] Department of Physics, Ahi Evran University, Kirsehir, Turkey

ARTICLE INFO

Article history:
Received 17 August 2010
Received in revised form 19 October 2010
Accepted 19 October 2010
Available online 26 October 2010

Keywords:
Dimethyl-2-(5-acetyl-2,2-dimethyl-4,6-dioxo-1,3-dioxan-5-yl)-3-(triphenylphosphinylidene)succinate
Infrared spectra
Density functional theory
Vibrational spectra
GIAO

ABSTRACT

Dimethyl-2-(5-acetyl-2,2-dimethyl-4,6-dioxo-1,3-dioxan-5-yl)-3-(triphenylphosphinylidene)succinate has been synthesized and characterized by elemental analysis, FT-IR and ^{1}H, ^{13}C and ^{31}P NMR. The vibrational wavenumbers, gauge including atomic orbital (GIAO) ^{1}H and ^{13}C chemical shift values of title compound in the ground state have been computed with density functional theory method (DFT) and the B3LYP functional. The basis sets used are 6-311G(d,p) and 6-31G(d). The harmonic vibrational wavenumbers have been computed and the scaled values have been compared with the experimental FT-IR spectra. The complete assignments have been performed on basis of the total energy distribution (TED) of the vibrational modes, calculated with scaled quantum mechanics (SQM) method. Most of the computed wavenumbers are found to be in good agreement with the observed spectrum.

1. Introduction

The phosphorus ylides represent an outstanding achievement of the chemistry of the 20th century [1]. These compounds have been found to be useful in a wide variety of reactions which are of interest to synthetic chemists especially in the synthesis of naturally occurring products and compounds with biological and pharmacological activity [2–5]. Developments of new protocols for synthesis of physiologically active compound have not been possible without phosphorus ylides. These compounds have attained great significance as widely used reagents for linking synthetic building blocks with the formation of carbon–carbon double bonds and development of new routes to heterocyclic systems [6–8]. Consequently much interest has been aroused in the study of the synthesis, structure and properties of P-ylides and their derivatives [9–11]. There are many studies involving the reaction between trivalent phosphorus nucleophiles and acetylenic esters in the presence of CH-acids [12]. However, in some cases, the ylide products cannot be isolated and appear to occur as intermediates on the reaction pathway leading to the observed product [13].

In this research we describe the synthesis of stabilized phosphorus ylide by the novel, one-pot and convenient reaction of dimethyl acetylenedicarboxylate (DMAD), triphenylphosphine (TPP) and Acyl Meldrum's acids. The sterically congested stabilized phosphorus ylide (**4**) is synthesized from the acetyl meldrum's acid (5-(1-hydroxyethylidene)-2,2-dimethyl-1,3-dioxane-4,6-dione) (3), TPP (1) and DMAD (2) (Scheme 1) [14].

The structures of product (**4**) were deduced from their elemental analyses, FT-IR, ^{1}H, ^{13}C and ^{31}P NMR spectral data. Stabilized phosphorus ylides have also been isolated from the related reactions of TPP, dialkyl acetylenedicarboxylate (DAAD) and cyclic and acyclic 1,3-diketones [15–20]. A plausible mechanism for the formation of ylides in this reaction is shown in Scheme 2.

The reaction starts from addition of TPP (1) to electron-deficient acetylenic ester (2) to form the zwitterionic intermediate (5) [21–23], which is subsequently protonated by the acid (3) to give vinyltriphenylphosphonium cation (**7**). Addition of the conjugate base of the acid (6)–(7) produces ylide (**4**) (Scheme 2).

Literature survey reveals that to the best of our knowledge the synthesis of compound (**4**) has not been reported. Thus, the aim of this study is to synthesise and characterise compound (**4**) and perform DFT/B3LYP computation and analysis. We hereby report our results.

* Corresponding author. Tel.: +98 2188848949; fax: +98 2188820993.
E-mail addresses: e_fereyduni@tmu.ac.ir, e_fereyduni@yahoo.com (E. Fereyduni).

0022-2860/$ - see front matter © 2010 Elsevier B.V. All rights reserved.
doi:10.1016/j.molstruc.2010.10.031

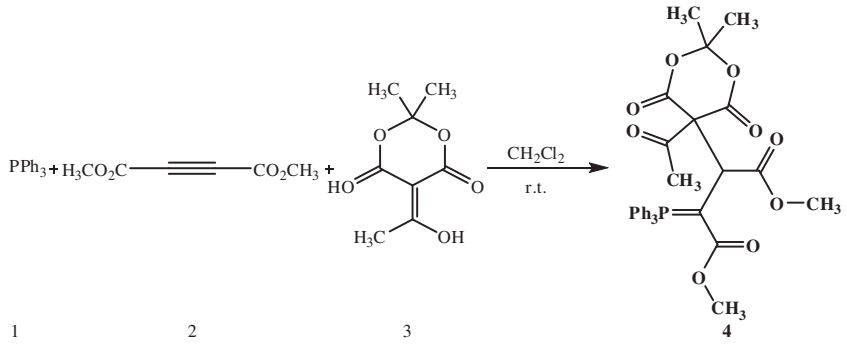

Scheme 1.

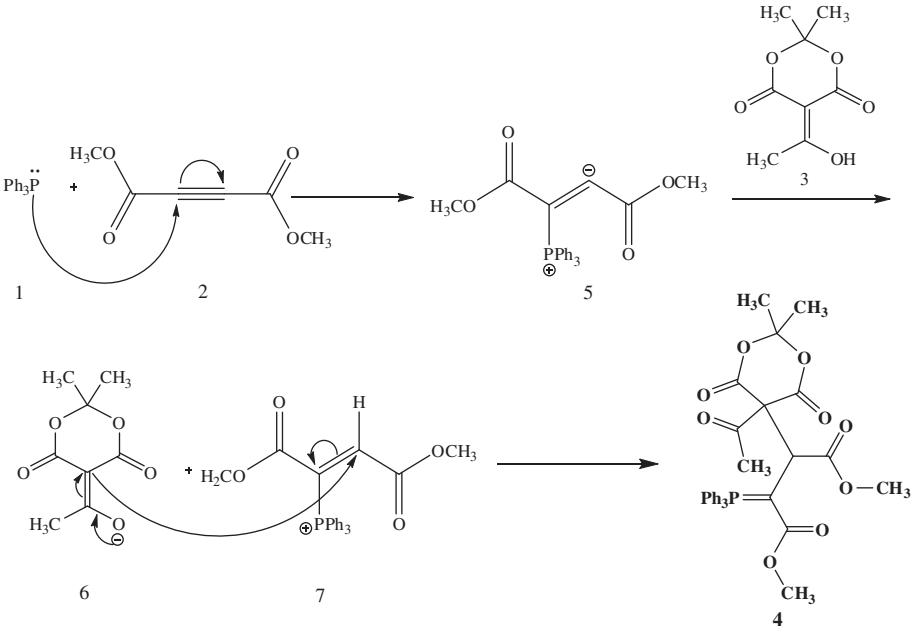

Scheme 2.

2. Experimental and theoretical methods

2.1. General method

^{1}H NMR (Fig. 1a), ^{13}C NMR (Fig. 1b) and ^{31}P NMR (Fig. 1c) spectra were recorded with Bruker Avance 300 spectrometer with the processing software XWIN-NMR version 3.1. Chemical shifts are reported on δ scale relative to TMS. IR spectra were recorded on a Perkin–Elmer spectrum RXI FT-IR spectrometer (400–4000 cm^{-1}; resolution: 1 cm^{-1}) using KBr discs. Elemental analyses were performed with Perkin–Elmer 2400 series II. Melting point was determined by Gallenkamp melting point apparatus.

2.2. Synthesis

The synthetic route is shown in Scheme 1. To a magnetically stirred solution of acetyl meldrum's acid (0.18 g, 1 mmol) and triphenylphosphine (0.26 g, 1 mmol) in CH_2Cl_2 (10 mL) a mixture of dimethylacetylenedicarboxylate (0.12 mL, 1 mmol) in CH_2Cl_2 (5 mL) was added drop wise at room temperature and the mixture was allowed to stirred for 1 h. The solvent was removed under reduced pressure and ylide (**4**) (0.57 g, m.p. (decompose) 137 °C, yield 97%) was obtained as an orange powder. FT-IR (in KBr pellet), υ (cm^{-1}): 1735 (C═O), 1667 (C═O), 1555 (C═O), 1303 (C—O), 1264 (C—O), 1190 (C—O), 1156 (C—O).^{1}H NMR (300.1 MHz, $CDCl_3$): δH = 1.67 (6H, s, $2CH_3$), 2.61 (3H, s, CH_3), 3.74 (6H, s, $2CH_3$), 6.81 (1H, s, CH), 7.39–7.64 (15H, m, 3Ph). ^{13}C NMR (75.47 MHz, $CDCl_3$): δC = 23.47 ($1CH_3$), 26.60 ($2CH_3$), 27.99 (CH), 42.55 (d, ^{1}JPC = 128.07 Hz, P═C), 52.11 ($2CH_3$), 91.59 (C(C═O)$_3$), 104.64 (C$(CH_3)_2$), 122.53 (d, ^{1}JPC = 99.02 Hz, C_{ipso}), 128.23–134.05 (C of Ph), 165.13 (C═O), 170.47 (C═O), 194.41 (C═O). ^{31}P NMR (121.49 MHz, $CDCl_3$): δP = 29.41 ppm. Analysis; calculated for $C_{32}H_{31}O_9P$: C, 65.08; H, 5.29; found: C, 65.17; H, 5.36%.

2.3. Theoretical methods

Gaussian 09 was used for computations and GaussView was used for molecular visualization [24]. The quantum chemical computations were performed using the DFT method and B3LYP functional. The basis sets used are 6-311G(d,p) and 6-31G(d). The geometry optimizations were followed by frequency calculations using same basis sets. The calculated frequencies were scaled and the scale factors used [25] are 0.967 (6-311G(d,p)) and 0.960 (6-31G(d)). The geometry of the title compound, together with that of tetramethylsilane (TMS) are fully optimized. ^{1}H and ^{13}C NMR chemical shifts are calculated within GIAO approach.

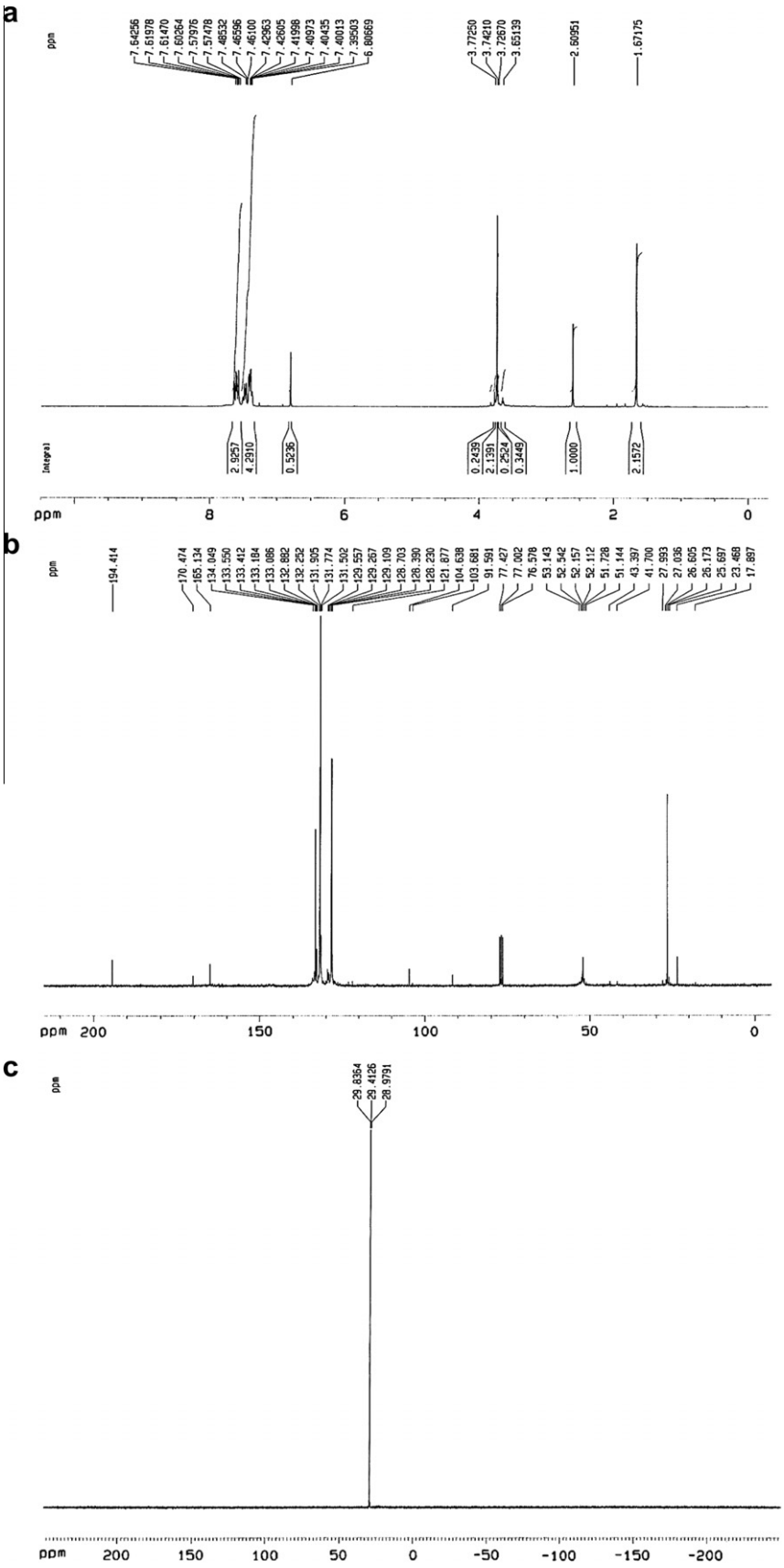

Fig. 1. (a) ^{1}H NMR spectra, (b) ^{13}C NMR spectra and (c) ^{31}P NMR spectra of (**4**).

3. Results and discussion

3.1. Geometrical structures

The selected optimized geometry parameters (bond lengths and angles) are listed in Table 1 along with the atom numbering given in Scheme 3. All optimized geometric parameters (bond lengths, angles and dihedrals for non-hydrogen atoms) are presented in Table S1 (Supplementary information). Since the crystal structure of compound (**4**) is not available, the optimized structure is compared with other analogous optimized compounds [26,27]. For example, the optimized bond length of C—C in the phenyl ring falls in the range 1.392–1.401 Å for the B3LYP/6-311G(d,p) method and 1.395–1.404 Å for the B3LYP/6-31G(d) method. This is in good agreement with an analogous molecule where the C—C bond length ranges from 1.359 to 1.387 Å [27]. Moreover, the predicted bond lengths of C_{11}—O_{12} (1.364 Å), C_{11}—O_{19} (1.197 Å) and C_{13}—O_{14} (1.435 Å) are in accord with the experimental values reported in Table 1. The optimized C_{ring}—P bond lengths (C_{25}—P, C_{31}—P and C_{37}—P) are 1.841 Å, 1.838 Å and 1.843 Å using B3LYP/6-311G(d,p) method and 1.840 Å, 1.837 Å and 1.843 Å using B3LYP/6-31G(d) method. However, these are slightly longer compared to a related molecular structure [27]. The B3LYP/6-311G(d,p) optimized C_{10}—C_{15}—O_{14}, C_{10}—C_{15}—O_{18} and O_{14}—C_{15}—O_{18} bond angles are 116.3°, 125.5° and 118.2° and these compare satisfactorily with the experimental angles 116.8°, 125.3° and 117.9° respectively.

3.2. Vibrational analysis

Atomic numbering scheme for the title compound is shown in Scheme 3. The molecule (**4**) consists of 73 atoms and therefore it has 213 normal vibrational modes. The observed vibrational assignments and analysis of (**4**) are discussed in terms of fundamental bands, overtones and combination bands. The FT-IR spectrum of (**4**) is shown in Fig. 2. Theoretical FT-IR spectra is reported in Fig. 3. The observed and calculated wavenumbers using B3LYP/6-311G(d,p) and B3LYP/6-31G(d) and total energy distribution (TED) of (**4**) are summarised in Table S2 (Supplementary information). The vibrational modes were assigned on the basis of TED analysis using SQM program [28]. A linear relation was found between experimental and theoretical frequencies (Fig. S1, Supplementary information). The correlation coefficients of regression procedure confirm the high quality of linear relations. As shown in Fig. S1 (Supplementary information), B3LYP/6-311G(d,p) computed values show better agreement with the experimental values.

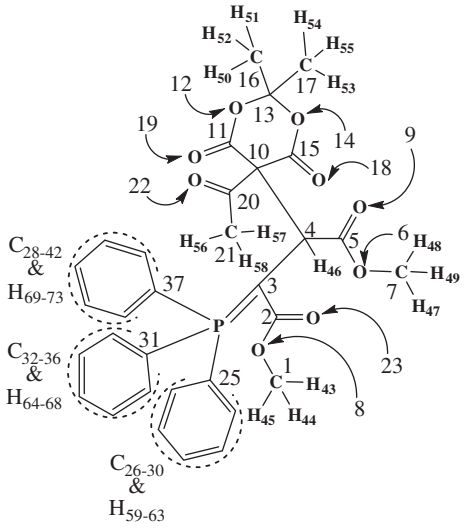

Scheme 3. Chemical structure of compound (**4**).

The aromatic structure shows the presence of the C—H stretching vibrations in the region 3000–3100 cm^{-1} which is the characteristic region for the ready identification of the C—H stretching vibrations [29]. The title compound has five C—H moieties corresponding to one phenyl ring, three C—H_3 and one C—H moieties as shown in Fig. 2. The wavenumber 3075 cm^{-1} is assigned to C—H stretching vibration of the phenyl groups. This peak is predicted at 3077 cm^{-1} (for B3LYP/6-311G(d,p)) and 3075 cm^{-1} (for B3LYP/6-31G(d)).

The C—H stretching vibrations of the methyl groups ($C_1H_{43-44-45}$, $C_7H_{47-48-49}$, $C_{16}H_{50-51-52}$, $C_{17}H_{53-54-55}$, $C_{21}H_{56-57-58}$) observed at 2954 cm^{-1} (2952 cm^{-1} for 6-311G(d,p)), 3019 cm^{-1} (3015 cm^{-1} for 6-311G(d,p)) and 3050 cm^{-1} (3049 cm^{-1} for 6-311G(d,p)) in the FT-IR spectra of the title compound. The 3050 cm^{-1} and 3019 cm^{-1} peaks are assigned to asymmetric CH stretching vibrations. Another peak (2954 cm^{-1}) is determined corresponding to symmetric CH stretching vibration.

The vibrational mode no. 188 is assigned to C_4—H_{46} stretching mode and is computed by B3LYP/6-311G(d,p) method to be 2991 cm^{-1}. This is in good agreement with recorded FT-IR data at 2986 cm^{-1}. All CH stretching vibrations are pure modes since their TED contribution is almost gives rise to ~98%. The obtained CH stretching wavenumbers are in good accord with the experimental data.

The most characteristic feature of carboxylic group is observed usually in the 1700–1800 cm^{-1} region [30]. This band is due to the C=O stretching vibration. This vibration is observed at 1735 cm^{-1} in the FT-IR spectra. The experimentally observed value of the C=O

Table 1
Selected geometrical parameters optimized in (**4**), bond length (Å) and bond angle (°).

Parameters	B3LYP/6-311G(d,p)	B3LYP/6-31G(d)	Exp. [26]	Exp. [27]
Bond length (Å)				
C_{10}—C_{11}	1.533	1.532	1.444	
C_{10}—C_{15}	1.539	1.539	1.438	
C_{11}—O_{12}	1.364	1.365	1.356	
C_{11}—O_{19}	1.197	1.204	1.205	
O_{12}—C_{13}	1.444	1.442	1.426	
C_{13}—O_{14}	1.435	1.434	1.439	
C_{13}—C_{16}	1.523	1.525	1.500	
C_{13}—C_{17}	1.522	1.525	1.505	
O_{14}—C_{15}	1.361	1.362	1.352	
C_{15}—O_{18}	1.195	1.202	1.210	
C_{31}—C_{32}	1.401	1.404		1.369
C_{31}—C_{36}	1.397	1.400		1.384
C_{32}—C_{33}	1.393	1.395		1.387
C_{33}—C_{34}	1.393	1.396		1.359
C_{34}—C_{35}	1.393	1.396		1.372
C_{35}—C_{36}	1.392	1.395		1.366
Bond angle (°)				
C_4—C_{10}—C_{11}	109.9	109.9	118.7	
C_4—C_{10}—C_{15}	109.4	109.4	120.7	
C_{10}—C_{11}—O_{12}	115.5	115.7	116.0	
C_{10}—C_{11}—O_{19}	125.5	125.5	125.8	
O_{12}—C_{11}—O_{19}	119.0	118.9	118.3	
C_{11}—O_{12}—C_{13}	123.1	122.9	118.4	
O_{12}—C_{13}—C_{16}	110.5	110.5	106.9	
O_{12}—C_{13}—C_{17}	105.7	105.7	109.8	
O_{14}—C_{13}—C_{16}	110.3	110.2	105.6	
O_{14}—C_{13}—C_{17}	105.7	105.7	110.3	
C_{16}—C_{13}—C_{17}	112.5	112.5	113.7	
C_{13}—O_{14}—C_{15}	125.1	124.9	118.3	
C_{10}—C_{15}—O_{14}	116.3	116.5	116.8	
C_{10}—C_{15}—O_{18}	125.5	125.5	125.3	
O_{14}—C_{15}—O_{18}	118.2	117.9	117.9	

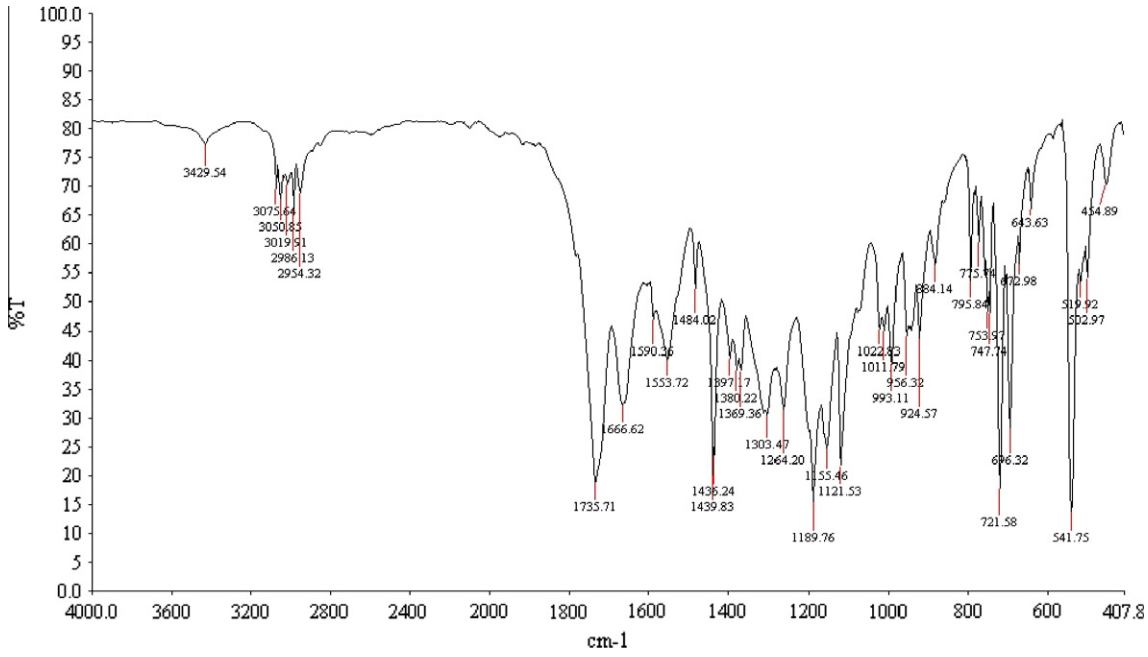

Fig. 2. FT-IR spectrum of (**4**).

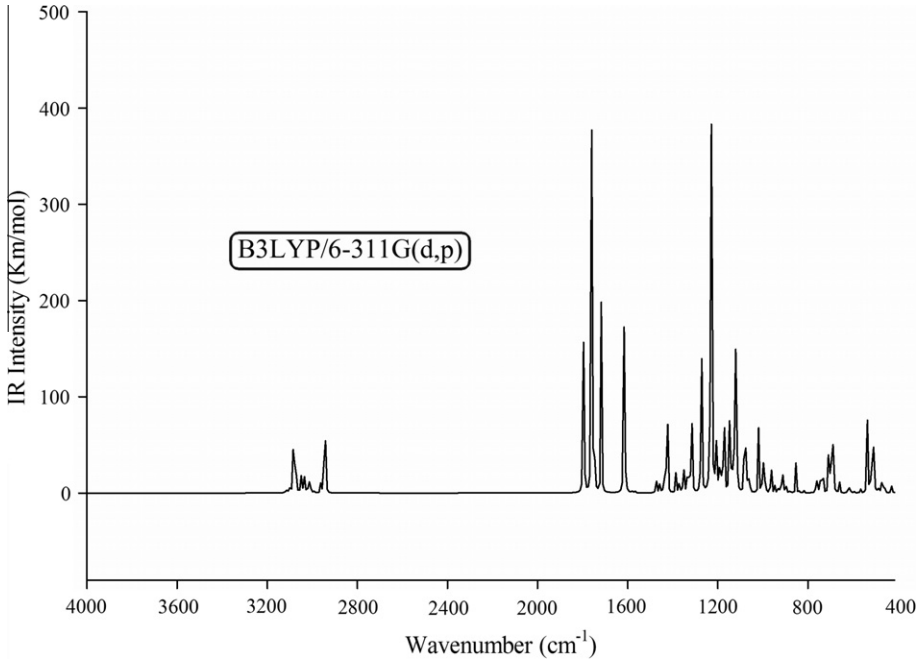

Fig. 3. Theoretical FT-IR spectrum of (**4**).

band shows very good agreement with computed values 1745 cm^{-1} and 1748 cm^{-1} at B3LYP/6-311G(d,p) and B3LYP/6-31G(d) levels of theory, respectively.

The ring carbon–carbon stretching vibrations occur in the region 1625–1430 cm^{-1}. In general, the bands are of variable intensity and are observed at 1625–1590, 1590–1575, 1540–1470, 1465–1430 and 1380–1280 cm^{-1} [31]. In the present work, the frequencies observed in the FT-IR spectrum are 1590, 1553, 1484, 1397 and 1303 cm^{-1} and they have been assigned to C—C stretching vibrations. The theoretically computed values, B3LYP/6-311G(d,p), at 1579, 1562, 1470, 1417 and 1310 cm^{-1} showing excellent agreement with experimental values.

In the FT-IR spectra of the title compounds vibration are assigned to the CH_3 scissoring vibrations at 1439 and 1436 cm^{-1}. These vibrations are predicted at 1435 and 1433 cm^{-1} using the B3LYP/6-311G(d,p) level of theory. The wagging vibrations of the CH_3 group are observed experimentally at 1380 cm^{-1} (1380 cm^{-1} for 6-311G(d,p)) and 1369 cm^{-1} (1365 cm^{-1} for 6-311G(d,p)) in the FT-IR spectra.

3.3. NMR spectra

^{1}H and ^{13}C NMR chemical shifts were calculated using the GIAO method [32] at the B3LYP/6-311G(d,p) and B3LYP/6-31G(d) levels.

The theoretical ^{1}H and ^{13}C NMR chemical shifts of (**4**) have been compared with the experimental data. According to these results, the calculated chemical shifts and coupling constants are in compliance with the experimental findings.

Table 2
Experimental and calculated ^{1}H and ^{13}C chemical shifts (ppm) of (**4**).

Chemical shifts	B3LYP/6-311G(d,p)		B3LYP/6-31G(d)		Exp.
H_{68}	8.54	7.60[a]–8.54[b]	8.72	7.78[a]–8.72[b]	7.39–7.64
H_{73}	8.36		8.54		
H_{66}	8.05		8.23		
H_{67}	8.00		8.18		
H_{72}	7.97		8.15		
H_{71}	7.91		8.09		
H_{59}	7.91		8.09		
H_{65}	7.90		8.08		
H_{61}	7.85		8.03		
H_{63}	7.79		7.97		
H_{70}	7.75		7.93		
H_{62}	7.74		7.92		
H_{69}	7.72		7.90		
H_{60}	7.68		7.86		
H_{64}	7.60		7.78		
H_{46}	6.87		6.15		6.81
H_{48}	5.34	3.54[c]	5.16	3.36[c]	3.74
H_{49}	3.91		3.73		
H_{43}	3.46		3.28		
H_{47}	3.43		3.25		
H_{45}	2.69		2.51		
H_{44}	2.41		2.23		
H_{57}	2.83	2.57[c]	2.79	2.50[c]	2.61
H_{58}	2.56		2.47		
H_{56}	2.32		2.24		
H_{50}	1.81	1.64[c]	1.99	1.82[c]	1.67
H_{54}	1.76		1.94		
H_{55}	1.67		1.85		
H_{52}	1.61		1.79		
H_{51}	1.56		1.74		
H_{53}	1.42		1.60		
C_{20}	194.78		213.43		194.41
C_{5}	172.85	170.97[c]	195.25	189.07[c]	170.47
C_{1}	169.08		182.88		
C_{11}	160.42	159.94[c]	171.90	171.09[c]	165.13
C_{15}	159.45		170.28		
C_{36}	132.54	119.44[a]–132.54[b]	157.26	132.77[a]–157.26[b]	128.23–134.05
C_{26}	129.92		144.18		
C_{30}	129.80		143.68		
C_{32}	127.55		141.21		
C_{38}	125.51		138.86		
C_{28}	125.18		138.81		
C_{34}	124.89		138.31		
C_{42}	124.56		137.95		
C_{40}	124.28		137.69		
C_{39}	121.74		135.15		
C_{35}	121.66		134.79		
C_{41}	121.26		134.74		
C_{27}	121.00		134.37		
C_{29}	120.77		134.03		
C_{33}	119.44		132.77		
C_{37}	126.90	123.42[c]	141.10	137.27[c]	122.53
C_{25}	122.97		136.59		
C_{31}	120.39		134.10		
C_{13}	105.12		113.19		104.64
C_{10}	93.46		99.54		91.59
C_{7}	54.67	52.98[c]	55.75	54.34[c]	52.11
C_{1}	51.30		52.93		
C_{3}	42.88		49.31		42.55
C_{4}	28.13		34.81		27.99
C_{17}	30.02	27.68[c]	33.21	30.59[c]	26.60
C_{16}	25.35		27.98		
C_{21}	21.13		25.26		23.47

[a] Minimum.
[b] Maximum.
[c] Average.

We have calculated ^{1}H chemical shift values (with respect to TMS) of 8.54–1.42 ppm and 8.72–1.60 ppm at B3LYP/6-311G(d,p) and B3LYP/6-31G(d), respectively, whereas the experimental shifts are observed at 7.64–1.67 ppm. The benzyl protons resonate as multiplet at 7.39–7.64 ppm experimentally and these have been predicted in the range 7.60–8.54 ppm and 7.78–8.72 at B3LYP/6-311G(d,p) and B3LYP/6-31G(d) levels of theory respectively. The CH_3 protons (C_{50-55}) of the title compound give a singlet at 1.67 ppm. This has been computed in the range of 1.42–1.81 ppm at B3LYP/6-311G(d,p) and 1.60–1.99 at B3LYP/6-31G(d) levels of theory. The singlet observed at 2.61 ppm is assigned to H_{56-58} and this has been computed to be in the range 2.32–2.83 ppm and

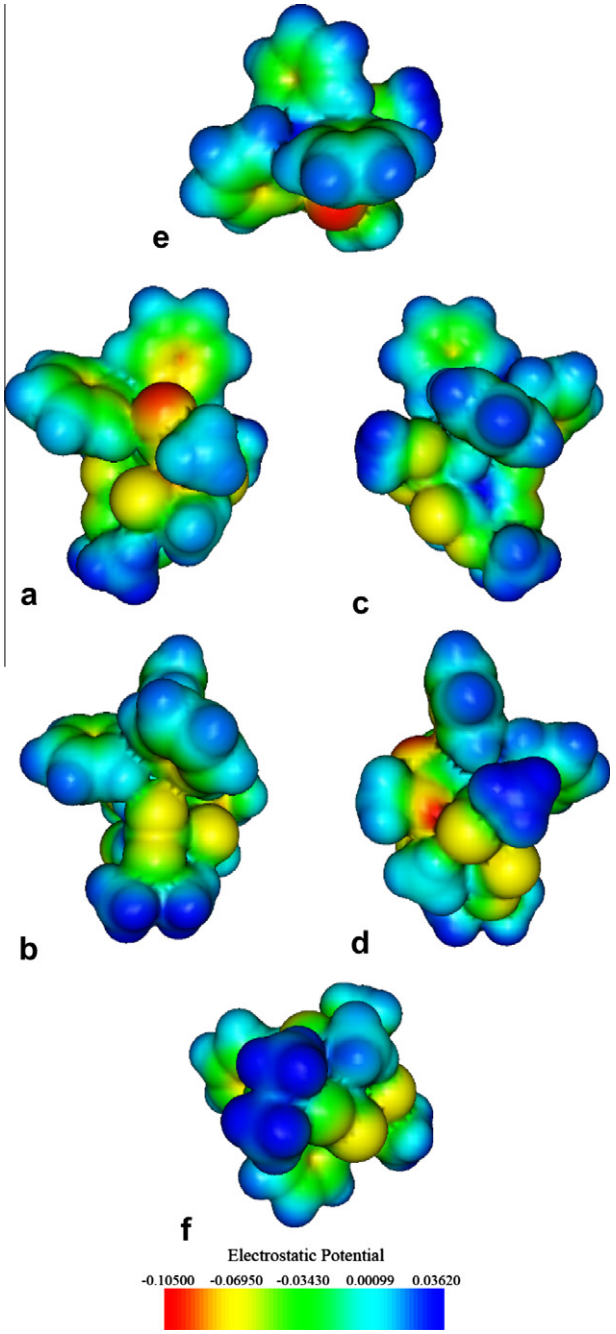

Fig. 4. B3LYP/6-311G(d,p) calculated 3D molecular electrostatic potential of (**4**) in various orientations, in a.u. (a: front, b: left, c: behind, d: right, e: top, f: bottom).

2.24–2.79 at B3LYP/6-311G(d,p) and B3LYP/6-31G(d) levels respectively. Complete ^{1}H NMR chemical shifts are given in Table 2.

^{13}C NMR spectrum of the title compound shows the signal at 23.47 ppm due to the C21 atom. This signal has been computed as 21.13 ppm at B3LYP/6-311G(d,p) and 25.26 ppm for B3LYP/6-31G(d) levels of theory. The signals at 27.99 and 42.55 ppm are assigned to C_4 and C_3 atoms, respectively and the computed values at B3LYP/6-311G(d,p) level are 28.13 and 42.88 ppm. The results of ^{13}C NMR calculations are tabulated in Table 2.

On comparing theoretical and the experimental data we obtain linear functions as follows:

For ^{1}H:

$y = 0.981x - 0.318$; $R^2 = 0.965$, B3LYP/6-311G(d,p),
$y = 0.941x - 0.126$; $R^2 = 0.955$, B3LYP/6-31G(d).

For ^{13}C:

$y = 1.031x + 0.497$; $R^2 = 0.992$, B3LYP/6-311G(d,p),
$y = 0.937x - 0.265$; $R^2 = 0.990$, B3LYP/6-31G(d).

As a result, the R^2 obtained for ^{13}C (0.992 and 0.990) are better than R^2 for ^{1}H (0.965 and 0.955). This discrepancy can be expected since the H shifts are more sensitive to solvent effects. According to these results, it is seen that the results of B3LYP/6-311G(d,p) are in better agreement to experimental data compared to B3LYP/6-31G(d).

3.4. Molecular electrostatic potential maps

The molecular electrostatic potential (MESP) is widely used as a reactivity map displaying most probable regions for the electrophilic attack of charged point-like reagents on organic molecules [33]. MESP contour map provides a simple way in predicting the interaction of different geometries. The electrostatic potential has been used primarily for predicting sites and relative reactivities towards electrophilic attack and in studies of biological recognition and hydrogen bonding interactions [34–40]. In order to predict the reactive sites for electrophilic and nucleophilic attacks of the title molecule, MESP was calculated at the B3LYP/6-311G(d,p) optimized geometry. The negative (red color)[1] regions of MESP were related to electrophilic reactivity and the positive (blue color) ones to nucleophilic reactivity shown in Fig. 4. As depicted in Fig. 4, this molecule has two possible sites for electrophilic attack. The negative regions are mainly over the O_8 and the partial region between O_9 and O_{23} atoms.

4. Conclusion

The stabilized phosphorus ylide (**4**) has been synthesized via the novel one-pot and convenient reaction of DMAD, TPP and acids such as Acyl Meldrum's acids. The structure was determined and characterized by elemental analysis, FT-IR, ^{1}H, ^{13}C and ^{31}P NMR. The vibrational frequencies and chemical shifts (^{1}H and ^{13}C) of the fundamental modes of the optimized geometry of (**4**) have been determined from DFT/B3LYP method. The geometry was optimized without any symmetry constraints with the 6-311G(d,p) and 6-31G(d) basis sets. Comparisons between the calculated vibrational wavenumbers and the experimental FT-IR spectra indicate that they support each other. To fit the theoretical vibrational wavenumber results with experimental data for B3LYP/6-311G(d,p), a scale factor of 0.967 has been used, whereas for B3LYP/6-31G(d) method the 0.960 scale factor was employed. However, the results of B3LYP/6-311G(d,p) method are in better agreement with the experimental outcome compared to the B3LYP/6-31G(d) level of theory.

[1] For interpretation of color in Fig. 4, the reader is referred to the web version of this article.

Acknowledgements

The author (Y. Erdogdu) would like to thank Ahi Evran University Research Fund for its financial support. Please acknowledge to Ms. Lydia Rhyman, who carefully reviewed my manuscript.

Appendix A. Supplementary material

Supplementary data associated with this article can be found, in the online version, at doi:10.1016/j.molstruc.2010.10.031.

References

[1] G. Wittig, Science 210 (1980) 600–604.
[2] O.I. Kolodiazhnyi, Russ. Chem. Rev. 66 (1997) 225–254.
[3] K.M. Pietrusiewiz, M. Zablocka, Chem. Rev. 94 (1994) 1375–1411.
[4] D.E.C. Cobridge, Phosphorus: An Outline of Chemistry, Biochemistry and Uses, fifth ed., Elsevier, Amsterdam, 1995.
[5] H.R. Hudson, Nucleophilic reactions of phosphines, in: F.R. Hartley (Ed.), The Chemistry of Organophosphorus Compounds, John Wiley & Sons, Chichester, 1990.
[6] I. Yavari, S. Asghari, M.M. Samadi-Zadeh, Iran. J. Chem. Chem. Eng. 17 (1998) 38–41.
[7] I. Yavari, S. Asghari, A.A. Esmaili, J. Chem. Res. (1999) 234–235.
[8] S. Asghari, A. Khabbazi-Habibi, J. Phosphorus Sulfur Silicon 180 (2005) 2451–2456.
[9] D.N. Nicolaides, D.R. Gautam, K.E. Litinas, T. Papamehael, J. Chem. Soc. Perkin Trans. 1 (2002) 1455–1460.
[10] D.N. Nicolaides, K.E. Litinas, A. Makri, V. Fragos, E. Galariniotou, Tetrahedron 63 (2007) 8298–8304.
[11] O.I. Kolodiazhnyi, Phosphorus Ylides, Chemistry and Application in Organic Synthesis, Wiley-VCH, New York, 1999.
[12] S. Asghari, M. Tajbakhsh, V. Taghipour, Tetrahedron Lett. 49 (2008) 1824–1827.
[13] P.J. Murphy, L.A. Evans, K.E. Griffiths, H. Guthmann, Tetrahedron Lett. 43 (2002) 299–301.
[14] A. Ramazani, A.R. Kazemizadeh, E. Ahmadi, K. Slepokura, T. Lis, Z. Naturforsch. 61b (2006) 1128–1133.
[15] A. Ramazani, M. Mohammadi-Vala, Phosphorus Sulfur Silicon Relat. Elem. 176 (2001) 223–229.
[16] A. Ramazani, L. Dolatyari, A.R. Kazemizadeh, E. Ahmadi, Asian J. Chem. 17 (2005) 297–300.
[17] I. Yavari, F. Nasiri, H. Djahaniani, Phosphorus Sulfur Silicon Relat. Elem. 178 (2003) 2627–2638.
[18] M.R. Islami, I. Yavari, A.M. Tikdari, L. Ebrahimi, S. Razee, H.R. Bijanzadeh, Russ. Chem. Bull. Int. Ed. 51 (2002) 2084–2087.
[19] I. Yavari, M.R. Islami, A. Habibi, A.M. Tikdari, L. Ebrahimi, Phosphorus Sulfur Silicon Relat. Elem. 179 (2004) 575–583.
[20] M.T. Maghsoodlou, S.M. Habibi Khorassani, N. Hazeri, M. Nassiri, Phosphorus Sulfur Silicon Relat. Elem. 181 (2006) 1363–1369.
[21] V. Nair, C. Rajesh, A.U. Vinod, S. Bindu, A.R. Sreekanth, J.S. Mathess, L. Balagopal, Acc. Chem. Res. 36 (2003) 899–907.
[22] L. Van Meervelt, R.N. Vydzhak, V.S. Brovarets, N.I. Mishchenko, B.S. Drach, Tetrahedron 50 (1994) 1889–1898.
[23] S.M. Habibi Khorassani, M.T. Maghsoodlou, A. Ebrahimi, H. Roohi, M. Zakarianezhad, J. Iran. Chem. Soc. 3 (2006) 223–232.
[24] M.J. Frisch, G.W. Trucks, H.B. Schlegel, G.E. Scuseria, M.A. Robb, J.R. Cheeseman, G. Scalmani, V. Barone, B. Mennucci, G.A. Petersson, H. Nakatsuji, M. Caricato, X. Li, H.P. Hratchian, A.F. Izmaylov, J. Bloino, G. Zheng, J.L. Sonnenberg, M. Hada, M. Ehara, K. Toyota, R. Fukuda, J. Hasegawa, M. Ishida, T. Nakajima, Y. Honda, O. Kitao, H. Nakai, T. Vreven, J.A. Montgomery Jr., J.E. Peralta, F. Ogliaro, M. Bearpark, J.J. Heyd, E. Brothers, K.N. Kudin, V.N. Staroverov, R. Kobayashi, J. Normand, K. Raghavachari, A. Rendell, J.C. Burant, S.S. Iyengar, J. Tomasi, M. Cossi, N. Rega, J.M. Millam, M. Klene, J.E. Knox, J.B. Cross, V. Bakken, C. Adamo, J. Jaramillo, R. Gomperts, R.E. Stratmann, O. Yazyev, A.J. Austin, R. Cammi, C. Pomelli, J.W. Ochterski, R.L. Martin, K. Morokuma, V.G. Zakrzewski, G.A. Voth, P. Salvador, J.J. Dannenberg, S. Dapprich, A.D. Daniels, O. Farkas, J.B. Foresman, J.V. Ortiz, J. Cioslowski, D.J. Fox, Gaussian 09, Revision A.02 Gaussian Inc., Wallingford, CT, 2009.
[25] http://cccbdb.nist.gov/vibscalejust.asp.
[26] R. Li, Z.-Y. Ding, Y.-Q. Wei, J. Ding, Acta Cryst. E65 (2009) o1296.
[27] O.V. Amirkhanov, I.O. Marchenko, O.V. Moroz, T.Yu. Sliva, I.O. Fritsky, Acta Cryst. E66 (2010) m640–m641.
[28] G. Rauhut, P. Pulay, J. Phys. Chem. 99 (1995) 3093–3100.
[29] Y. Erdogdu, M.T. Gulluoglu, M. Kurt, J. Raman Spectrosc. 40 (11) (2009) 1615–1623.
[30] N. Sundaraganesan, B. Dominic Joshua, C. Meganathan, R. Meenashi, J.P. Cornard, Spectrochim. Acta A 70 (2) (2008) 376–383.

[31] G. Varsanyi, Vibrational Spectra of Benzene Derivatives, Academic Press, New York, 1969.
[32] K. Wolinski, J.F. Hinton, P. Pulay, J. Am. Chem. Soc. 112 (1990) 8251–8260.
[33] P. Politzer, D.G. Truhlar (Eds.), Chemical Application of Atomic and Molecular Electrostatic Potentials, Plenum, New York, 1981.
[34] E. Scrocco, J. Tomasi, Adv. Quantum Chem. 11 (1978) 115–121.
[35] C. Muñoz-Caro, A. Niño, M.L. Sement, J.M. Leal, S. Ibeas, J. Org. Chem. 65 (2000) 405–410.
[36] P. Politzer, K.C. Daiker, The Force Concept in Chemistry, Van Nostrand Reinhold Co., 1981.
[37] P. Politzer, P.R. Laurence, K. Jayasuriya, in: J. McKinney, Structure Activity Correlation in Mechanism Studies and Predictive Toxicology, Special Issue of Environ. Health Perspect., vol. 61, 1985, p. 191.
[38] P. Politzer, J.S. Murray, in: D.L. Protein, R. Beveridge, R. Lavery (Eds.), Theoretical Biochemistry and Molecular Biophysics: A Comprehensive Survey, vol. 2, Adenine Press, Schenectady, NY, 1991, pp. 165–191.
[39] E. Scrocco, J. Tomasi, Topics in Current Chemistry, vol. 42, Springer Verlag, Berlin, 1973.
[40] P. Politzer, D.G. Truhlar (Eds.), Chemical Applications of Atomic and Molecular Electrostatic Potentials, Plenum Press, NY, 1981.